International Journal of Sciences: Basic and Applied Research (IJSBAR)

ISSN 2307-4531
(Print & Online)

http://gssrr.org/index.php?journal=JournalOfBasicAndApplied

Spectroscopic Characterization, Thermal Behavior, Surface Activity and Docking Studies of Synthesized Orthohydroxyacetophenone Azine Ligand and its Complexes with Pd (II) and Mn (II)Ions

I.A. Ibrahem[a], E. F. Abo Zeid[b*]

[a]*Chemistry Department, Faculty of Science, Al Azhar University, Nasr City, Cairo, 11884,Egypt*

[b]*Physics Department, Faculty of Science, Assiut University, Assiut 71516, Egypt*

[a]*Email: foribrahem@yahoo.com*

[b]*Email: esabozaid@yahoo.com*

Abstract

The complexes of Pd(II) and Mn(II) with orthohydroxyacetophenone azine ligand have been prepared and characterized by spectroscopic data, magnetic moment, thermal and SEM measurements. The data of the samples suggest that the ligand sites are one water molecule, imino nitrogen and two phenolic oxygens coordinated to the Pd (II) ion and N2O2 with water molecules to the Mn(II) ion. Geometrical structure of the complexes using molecular structural studies showed the square planar and octahedral for Pd (II) and Mn (II) complexes respectively. Geometry of the complexes confirmed using ESR spectra and thermal analysis. Molecular docking studies of the complexes with dihydrofolate reductase (DHFR) enzyme has been determined. The observed activity of Pd(II) complex gave rise to the conclusion that they might exert their action through inhibition of the DHFR enzyme. This behavior of Pd (II) complex confirmed by the highly active surface area which obtained from the XRD data.

Keywords: Spectroscopic characterization; Azines; Thermal Behavior; Docking; Surface Activity.

---

* Corresponding author.

1. Introduction

Pd (II) and Mn(II) complexes have been synthesized from orthohydroxyacetophenon azine ligand. Azines are compounds resulting from the reaction of two molecules of identical carbonyl compounds (symmetrical azines) or, from the reaction of two different carbonyl compounds (unsymmetrical azines) with hydrazine. According to whether the carbonyl compound is an aldehyde or a ketone, azines are called aldazines or ketazines, respectively. Azines that are N–N-linked di imines are 2, 3-diaza analogs of 1, 3-butadiene. The two imine bonds that form the azine moiety may be considered as polar acceptor groups oriented in opposite directions, as they include an N–N bond. On the basis of their relationship to butadiene, electronic delocalization may be expected. Using the advantage of reactivity of transition-metal complexes has attracted considerable interest to develop new systems in organic synthesis. Due to their ability to donate from two to eight electrons via lone pairs of the N atom and the C=N p-orbital electrons, azines show a highly ability in the binding to metal centers for the complexes formation. The large activity of the azines compounds from their analogy with Schiff base considered in the several application [1-5].

Transition metal complexes of Pd (II) and Mn (II) have been amongst the most widely studies of coordination compounds in the past few years, since they are found to be of importance as analytical and antimicrobial agents [6, 7]. Considerable efforts have been made to study the behavior and functions of palladium and manganese in biological system as well as in catalytic and pharmaceutical applications [8-10] and recently used as probe for assessment for α – amalyse activity in human saliva [6]. The biological activities of the transition metal complexes have been found to be generally dependent on the feature of the metal ions such as, oxidation state, and types of the coordinated ligand [11]. One of the most dangerous diseases in recent years is cancer where uncontrolled pathological proliferation of cell due to unspecific division of normal cell [12, 13]. Cancer chemotherapy is facing some challenges due to their severe side effect [14] as a result of production free radicals and reactive oxidant species [15, 16]. Due to the above fact, efforts focused on the design of drugs that can avoid these problems [17]. In the present work the spectral study is presented for Mn (II) complex using FTIR, electronic absorption spectra, and magnetic moment, while oOH acetophenone azin ligand and its complex with Pd (II) are previously studied [6, 18]. The crystal structure and active surface area of the complexes can be determined using X- ray diffraction (XRD). Scanning Electron Microscope (SEM) used to detect the morphology structure of the complexes, thermal analysis, thermodynamic parameters, and decomposition kinetics of the complexes using TGA and DTA instrument. Finally, the energy minimized structure of the ligand and its complexes have been obtained using Molecular Operating Environmental (MOE) and has been used to molecular docking study with (DHFR) enzyme to suggest the most probable mode of interaction of the samples with the selected enzymes.

2. Experimental

2.1. Synthesis of the ligand

The orthohydroxyacetophenone azine ligand was prepared using a previously described method [18] by the reaction of (0.1mole, 13.6 gram) of orthohydroxyacetophenone dissolved in 95% ethanol solvent with (0.05 mole, 2.5 gram) of hydrazine hydrate dissolved in the same solvent. The reaction mixture was heated with

refluxed for one hour. Cooling to room temperature produced yellow crystals which were filtered and recrystallized from ethanol.

2.2. Synthesis of the Metal ion Complexes

The Pd (II) complex was prepared according to the method described in the literature [1], while Mn (II) complex was prepared by adding a hot solution of (0.1mole) MnCl2.4H2O dissolved in 50 ml DMF solvent to a solution of ligand (0.1mol) dissolved in 50 ml DMF with stirring. The complex were formed and settled down on standing. The complex was filtered, washed with DMF and dried in air and stored in an air light sample bottle. The product complex exhibit a reddish brown color.

2.3. Physical Methods of Measurements

All chemicals used were of the analytical reagent grade (AR), and of heist purity available. Organic solvents used included absolute ethanol and dimethylformamid (DMF). These solvents were spectroscopically pure from BDH. The FTIR spectra of the ligand and its complexes in the range 4000-400 cm-1 were recorded with a Perkin Elmer spectrum RXI FTIR system scans at 2 cm-1 resolution. All IR measurements were carried out at room temperature using KBr disks. The ultraviolet and visible absorption spectra of the ligand and its metal complexes were recorded in DMF solvent using a Perkin Elmer spectrophotometer in the region of 200-800 nm. X-Band ESR spectra of the Mn(II) complex were recorded at room temperature on a Varian ESR-E 112 spectrometer. DPPH (2, 2′- biphenyl -1-picrylhydrazyl) with g value 2.0323 was used as the standard g marker. The XRD measurements of the complexes were performed using a broker axs, D8 advance. The pattern were run with Ni-filtered copper radiation (λ=1.5404A°) at 40 keV and 40 mA, with a scanning speed of 2θ=2.5˚/min. The XRD spectra were obtained using high resolution in the step-scanning mode with a narrow receiving slit (0.02°). XRD patterns were recorded in the 2h range of 5–70°. Scherrer's equation was employed to estimate particle size from XRD. Thermal analysis, thermodynamic parameters and decomposition kinetics were performed to follow the changes of weight of the specimens with temperature of a powder sample of about 5.5 mg was prepared, the specimen was studied at a heating rate of 10 K/min from room temperature up to about 750 K. The instruments used for performing DTA and TGA analysis were DO 8T-12 TG 01(SHIMADZU, JAPAN). The morphology of samples was observed using Scanning Electron Microscopy (SEM, JEOL- JSM-T 330A) with an acceleration voltage 30 keV. All of the images were recorded with a charge-coupled device camera.

2.4. Molecular Docking

Thymidylate synthase and dihydrofolate reductase are among the main targets involved in anticancer and antimicrobial activity [19, 20]. A molecular modeling study using the Molecular Operating Environment (MOE) [21] module was performed in order to rationalize the observed anticancer activity of ligand and its complexes. Molecular docking studies further helped in explaining the mode of action of the compounds through their various interactions with the active sites of the dihydrofolate reductase (DHFR) enzyme.

3. Results and Discussion

3.1. Characterization of the Ligand and its Complexes

3.1.1. IR Spectra of the ligand and its complexes

IR spectra of the ligand and its complexes were recorded in 4000-400 cm-1 range using KBr pellets table 1. Ligand and Pd (II) complex are previously assigned [1, 18]. The ligand showed the smaller of the bands reflected to symmetric nature of the molecule [18]. The medium broad band at 3430 cm-1 was attributed to (υ OH) disappears in the Mn (II) complex and a new band appeared at 3500 cm-1 assigned to (υ OH) of the water molecules, coordinated during complexation. The (υ C=N) stretch is observed at 1605 cm-1 with a very strong intensity, this band shift to higher wave number in the Mn (II) complex. This litter shift trend was previously found for salen complexes. This indicates that the ligand is coordinated through its imine group [22]. The strong band is showed at 1300 cm-1 was assigned to presence of (υ O-ph) [18], this mode stretch as the major coordinate shifts to 1387cm-1 in the complex formation [22, 23]. In addition to the above the IR spectra of the metal chelates shows absorption bands at 683 cm-1 and 459 cm-1 are due to (υ M-O) and (υ M-N) respectively [22].

Table 1: Assignment of the IR spectra (cm^{-1}) of the ligand and its complex with Mn (II)

Compound	υ (OH)	υ (C=N)	υ (O-Ph)	υ (C-(CH_3)Ph)	υ (M-O)	υ (M-N)
Ligand	3430	1605	1300	1247	-	-
Mn(II) complex	3500	1624	1387	1277	459	683

3.1.2. The UV/Visible spectra

The electronic absorption spectra of the ligand and Pd (II) complex are previously assigned [1, 18]. Orthohydroxyacetophenone azine ligand showed three bands at 282, 325 and 362 nm in DMF which are attributed to π –π* (1 Bu – 11Ag) and n-π* (1Au - 11Ag). The octahedral manganese (II) complex was brown. This color is a guide to confirm that the formed Mn (II) complex has octahedral geometry rather than tetrahedral [12, 23]. In the UV- Visible spectra of Mn (II) complex figure. 1, the bands related to π –π* and n- π* transition of the ligand disappears and new bands appears at 328 and 378 these bands assigned to LMCT transition, another band appeared at 405 nm due to d-d transition corresponding to the 3A1g-3T1g electronic state indicating octahedral geometry structure [17]. The octahedral Mn (II) complex gives an essentially spin-only magnetic moment value of 5.60 B. M., which does not vary much since the magnetic moment is temperature independent. The observed magnetic moment value 5.60 B.M. in Mn(II) complex is appreciably close to the calculated spin value [12,17]. The values of the electronic spectrum, magnetic moment and proposed structure of the compounds showed in table 2.

3.1.3. ESR spectrum

The ESR spectra of Mn (II) complex figure 2 were recorded on X-band frequency (9.5 GHz) under magnetic field strength of 3447 G at room temperature. The g value was determined using the relation $E = g\mu_\beta B_\circ$. Where

E the energy, g proportionality factor, μ_β Bohr magneton and $B_\circ$ external magnetic field. The spectrum of Mn (II) complex show a strong broad signal with g value 1.81 and 2.13 for $g_\perp$ and $g_\parallel$ respectively. The value of $g_{eff.}$ was found as 3.69 which are characteristic for octahedral high spin Mn (II) complex. The positive deviation of g_{eff} from the value of the free electron 2.0023 can be ascribed to partial increased covalent nature of the bonding between Mn (II) and the ligand molecule [8-24]. The Mn (II) complexes are of high spin variety, exhibiting magnetic moment values of 5.60-5.62 B. M., which corresponded to the octahedral geometry structure of the complexes [17]. Hence, based on spectroscopic studies the proposed structure of the Mn (II) complex is expected to be octahedral structure with coordination through the two oxygen atoms, two nitrogen atoms of the azomethin group and two water molecule scheme 1.

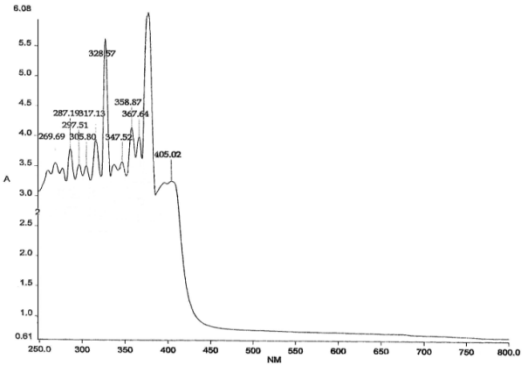

Figure 1: UV-Vis spectra of Mn(II) complex

Table 2: UV-Vis spectra, magnetic moment and proposed structure of the ligand and its complex with Mn (II)

Compound	UV-Vis spectra(nm)	Magnetic moment	proposed structure
Ligand	282, 325, 362	-	-
Mn (II) complex	328,378,405	5.60	octahedral

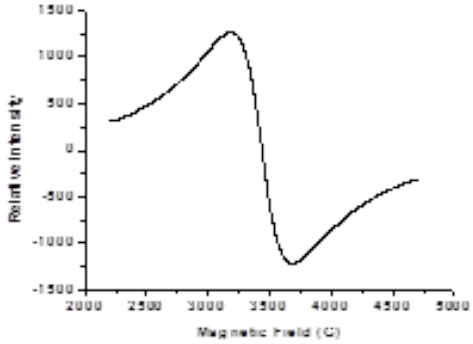

Figure 2: X-band ESR spectrum of Mn (II) complex

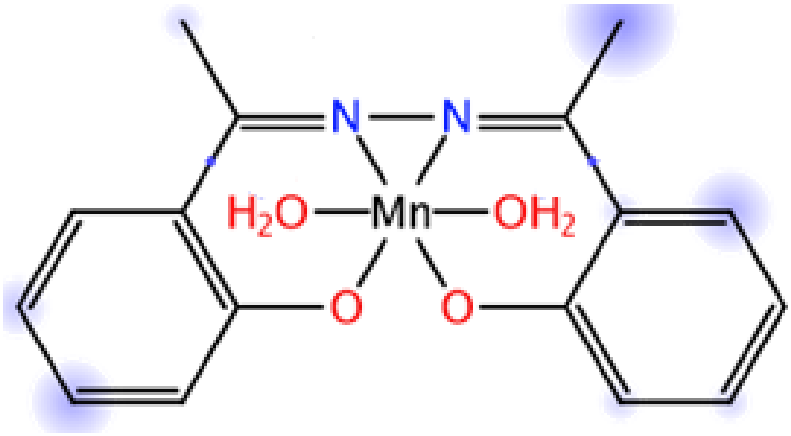

Figure 9: Scheme 1: The proposed structure of Mn (II) complex

3.2. Thermal analysis

3.2.1. Thermal decomposition of the ligand and its complexes

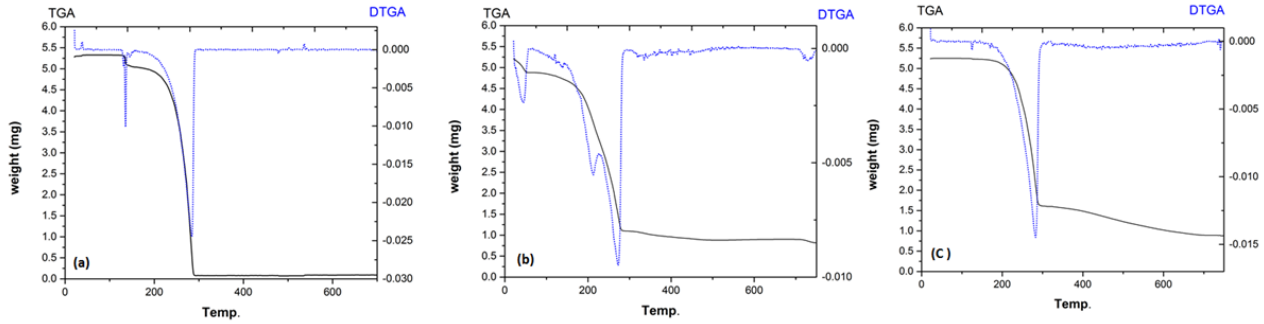

Figure 3: TGA and DTGA curves of (a) ligand, (b) Pd(II) and (c) Mn(II) complexes

Thermogavemetric analysis (TGA) and differential thermal analysis (DTA) are useful technique to determine the thermal stability of the metal complexes. In the present study, heating rate was suitably controlled at 10 °C / min under nitrogen atmosphere and the loss of weight was measured up to750 °C. the stages of decomposition temperature range, decomposition product and weight loss percentage of the samples are given in table 3. The proposed formula for all the compounds are confirmed by TG curves and the corresponding weight losses for each step of decomposition reaction of the ligand and its complexes are shown in figure 3.

The Schiff base ligand exhibits a first estimated mass loss of 3.95% (calc. 5.50%) at 125 °C -168°C, which may be ascribed to losses of the methyl group. In the following stages within the temperature range from 168°C-295°C the organic part $C_{15}H_{13}N_2O_2$ are lost with an estimated mass loss 95.72% (calc. 94.40%). The TG curve of Palladium complex shows four stages of decomposition within the temperature range 20 °C - 750 °C. The first mass loss is due to losses the methyl groups which occurs between 20°C -77°C, and has loss of 6.05% (calc. 6.50%), then the coordinated water, the organic moity without methyl groups and two chlorine atoms decomposed in the second and third stages between 78 °C and 281 °C with mass loss of 76.81% (calc. 75.40%). The residue of Pd metal decomposed during the end of the final stage from 282 °C to 750 °C with mass loss of

1.3% (calc. 1.00%). The overall weight loss amounts to 84.16% (calc. 82.9%).

The thermogram of Mn (II)-L chelate show two decomposition steps within the temperature range from 168 °C – 750 °C. The first step of decomposition within the temperature range 168 °C – 297 °C corresponds to losses of two coordinated water molecules, chlorine atoms + $C_{11}H_{14}N_2O$ with an estimated mass loss of 69.05% (calc. 69.39%). While final step occurs within the temperature range from 298 °C – 750 °C which corresponds to the removal of the oxygen atom leaving the metal and residual carbon with an estimated mass loss of 14.41% (calc. 12.21%). The overall weight loss amounts to 83.49% (calc. 81.60%).

Table 3: Thermal decomposition data of the ligand and its metal complexes

Compound	TG range	DTG_{max} (°C)	n*	Mass loss% obs.(calc.)	Total mass loss (%)	Assignment	Residue
L	125-168	408	1	3.95 (5.50)		CH_3 group	
	168-295	546	1	95.72 (94.40)	99.67(99.90)	loss of $C_{15}H_{13}N_2O_2$	-
Pd (II)	20-77	317	1	6.05 (6.50)		CH_3 Groups	
Complex	78-228	487	1	72.63		Coordinated water + Remaining organic Moity + chlorine atoms	
	229-281	545	1	4.18(75.40)	84.16(82.90)		
	282-750	608	1	1.30 (1.00)		Pd	-
Mn (II) Complex	168-297	281	1	69.05(69.39)		Two coordinated water + chlorine atoms +$C_{11}H_{14}N_2O$	
					83.49(81.60)		Mn metal + residual Carbon
	298-750	717	1	14.44(12.21)		Oxygen atom	

n*=number of decomposition steps

3.2.2. Kinetic parameters

The thermodynamic activation parameters of decomposition processes of the samples the activation energy (E*), enthalpy (H*), entropy (S*) and Gibbs free energy change of the decomposition (G*) were evaluated graphically by using the Coats-Redfern equation [25].

$$Log\left[\frac{g(\alpha)}{T^2}\right] = log\frac{AR}{\varphi E}\left[1-\frac{2RT}{E}\right] - \frac{E}{2.303RT} \qquad (1)$$

Where, $g(\alpha) = \log[\frac{W_\infty}{W_\infty - W}]$ [26] where W∞ is the mass loss at the completion of the decomposition reaction, W is the mass loss up to temperature T, R is the gas constant and φ is the heating rate. Since 1 - 2RT/E* ≈ 1, the

plot of the left-hand side of Eq. (1) against 1/T would give a straight line. E* was then calculated from the slope and the Arrhenius constant, A, was obtained from the intercept. The other kinetic parameters; the entropy of activation (S*), enthalpy of activation (H*) and the free energy change of activation (G*) were calculated using the following equations [26-28]:

$$s = 2.303\left(log\frac{Ah}{KT}\right)R \quad (2)$$

$$H^* = E^* - RT \quad (3)$$

$$G^* = H^* - TS^* \quad (4)$$

Where (k) and (h) are the Boltzman and Planck constants, respectively. The various kinetic parameters calculated are given in Table 4. The activation energy (E) in the different stages are in the range 296.21072 - 244627.21 kJ mol−1. The high values of the activation energies reflect the highly thermal stability of the complexes. The data of the entropy of activation was found to have negative values in all stages of the decomposition of samples except the second and third stage in the ligand and Pd(II) complex respectively. The negative values indicate that the decomposition reactions proceed with a lower rate than the normal ones, where the positive value indicates the higher rates of decomposition reactions. There is no definite trend either in the values of A or S among the different stages in the present series.

Table 4: Kinetic parameters for the thermal decomposition of the ligand and its metal complexes

Compound	Stage	E^*(KJ mol^{-1})	S^* (J mol^{-1})	A (S^{-1})	H^*(J mol^{-1})	G^*(J mol^{-1})
Ligand	I	119378.17	-2.574682	6.25 E+12	115979.45	117031.2
	II	244627.21	275.29874	2.72E+27	240079.5	89601.207
Pd(II)	I	454.5879	-192.4252	5.89E+02	-2182.852	58815.95
	II	51120.103	-167.9182	1.72E+04	47068.263	128844.43
	III	323616.2	363.6198	1.11E+32	319081.8	120909.01
	IV	363.77797	-314.7944	4.59E-04	-4694.782	186700.23
Mn(II)	I	553.36818	-72.28805	1.94E+09	-4055.912	35991.667
	II	296.21072	-277.2934	4.92E-02	-5669.229	193150.11

3.3. Scanning Electron Microscopy (SEM)

Surface images using SEM (Figure 4) demonstrate to the structures of the surface of prepared orthohydroxy acetophenon azine ligand and its complexes. Analysis of these images shows the size of pores to be quite different between the ligand and its metal complexes. SEM examination where checked the surface structure of the ligand which indicates a microcrystalline structure with hexagonal shape. The SEM micrographs of metal complexes shows an elongated and highly dispersed particles that form large agglomerates in which narrow distributed particles are uniformly distributed in the crystalline lattice of the ligand. The difference between the morphology structures indicates the formation of the metal complexes.

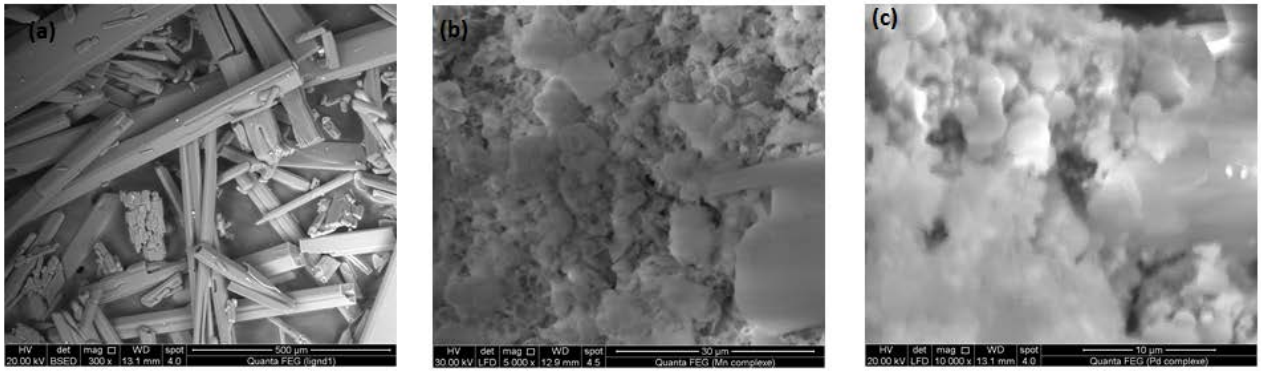

Figure 4: SEM pictures of (A) Ligand, (B) Mn(II) and (C) Pd(II) Complexes

3.4. X-ray Powder Diffraction

The x-ray powder diffraction patterns for the powder orthohydroxyacetophenone azine Schiff base ligand and its complexes with Pd (II) and Mn (II) metal ions are depicted in Figure 5. Inspection these patterns, we notice that the systems are well crystalline in the case of the ligand and semi-crystalline in the case of its complexes. The average particle size of the ligand and its complexes were calculated by employing the Deby-Scherer equation

$$\boldsymbol{D(A^{\circ}) = k\,\lambda\,/\,(\beta\,cos\,\theta\,)}\text{[27]}, \qquad (5)$$

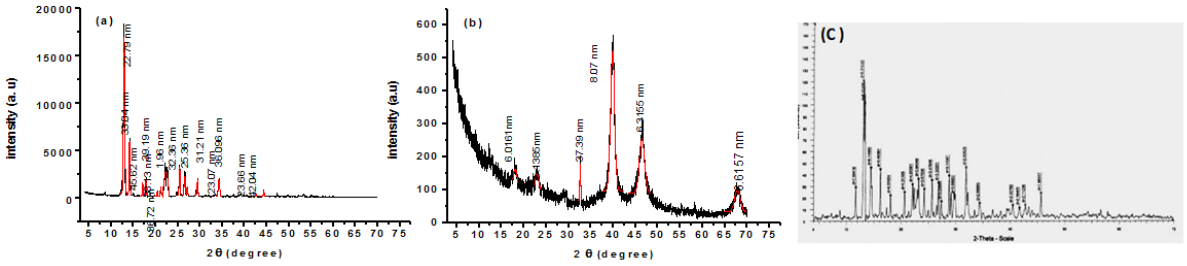

Figure 5: XRD spectra of (a) organic ligand, (b) Pd (II) complex and (C) Mn(II) complex

where D is the average particle size in A°, k is a shape sensitive coefficient (0.94), λ is the wavelength of radiation used Cu Kα (1.54056 A°), β is the full width half maximum (in rad) of the peak and θ is the angle at the position of peak maximum (in rad). The definite diffraction data like angle (2θ˚), interplanar spacing (d value, Angstrom), and relative intensity (%) have been calculated. The values of 2θ˚, d value (the volume average of the crystal dimension normal to diffraction plane), full width at half maximum (FWHM) of prominent intensity peak, relative intensity (%) and particle size of Paladium and Manganez complexes were estimated at the preferred planes as indicated in the table 5. The particle size was estimated according to the highest value of intensity compared with the other peaks. These data gave an impression that the particle size of the ligand and its Pd (II) complex located within nano-scale range. The pattern (Figure 5) corresponds to a single-phase orthohydroxyacetophenone azine of the monoclinic system with preferred orientation, where the (020) reflecting plane is the predominant plane. The lattice parameters were determined by introducing the X-ray data produced by the X-ray diffractometer into a treor X-ray program and were found to be a=1.578 nm,

b=1.394 nm, c=0.647 nm. The plane angles were found to be α= γ = 90˚ and β= 123.8˚ [1].

The Rhombohedral system with preferred orientation with (202) reflecting plane for Pd (II) and Mn (II) complexes were obtained. The lattice parameters were found to be a=5.494 nm, b= 5.494nm and c= 13.410 nm. The plane angles were found to α= β= 90˚and γ = 120˚ for each complex.

The particle surface area S in $m^2\ g^{-1}$ was calculated using the equation S = 6000/dρ for spherical particles [28], where d is the crystallite size (diameter) in nm obtained from the (020) and (202) diffraction lines for the ligand and Pd (II), Mn (II) complexes respectively, XRD data (Figure 5), and ρ is the density of the compounds (≈6.05 g cm^{-3}). This equation is obtained by dividing the surface area of a spherical particle (4 π r^2) by the mass of the spherical particle (mass = density x volume = ρ x 4 π r^3/3), where r is the radius of the spherical particle (d/2). To make appropriate changes obtaining the surface area value in $m^2\ g^{-1}$, the density and crystal size values are substituted, respectively, in g cm^{-3} and nm. The values of the surface activity of the orthohydroxyacetophenone azine and its complexes listed in the table 5.

Table 5: Active surface area (S m^2g^{-1}) and particle size (D nm) of the ligand and its complexes

Compound	Ligand	Pd(II) complex	Mn(II) Complex
S (m^2g^{-1})	20.967	78.709	11.110
D (nm)	47.3	12.6	89.3

From the data in the table we can conclude that, the addition of Pd (II) metal to the ligand to syntheses the complex increases the active surface area, where the addition of the Mn (II) metal decreases it.

3.5. Docking studies with DHFR

The three dimensional co-crystal structure of dihydrofolate reductase combined with the potent inhibitor, methotrexate (PDB ID: 4DFR). Scheme 2 thus illustrates the representative keys for the type of interaction between substrates and the enzyme, which can be used as a guide in the docking in Figures 6-8.

MOE (Molecular Operating Environment) docking studies of the inhibitors were performed using Ligand with DHFR enzyme active sites (figure 6) revealed that hydrogen bond beside hydrophobic interactions were considered responsible for the observed affinity as it acts as a pi-H hydrogen bond to Ile 7 backbone (2.84 Å) residues. This exists alongside many hydrophobic interactions with various amino acid residues: Phe 34, Ile 16, Leu 22, Gly 17, Thr 146, Asp 21, Thr 56, Gly 20, Ser 59, Gly 117, Val 8 and Ala 9.

Docking of Pd (II)complex into the DHFR active site (figure 7) revealed that hydrogen bond interactions beside hydrophobic interactions were considered responsible for the observed affinity as it acts as H hydrogen bond to Ser 59 (2.98 Å) sidechain residues. This exists alongside many hydrophobic interactions with various amino acid residues: Ile 16, Gly 116, Thr 146, Val 115, Val 8, Ile 7, Phe 34, Phe 31, Thr 56 and Gly 20.

Docking of Mn (II) complex into the DHFR active site (figure 8) revealed that hydrogen bond interactions

beside hydrophobic interactions were considered responsible for the observed affinity as it acts as H hydrogen bond to Val 115 (2.95 Å) and Ile 16 (2.88 Å) backbone residues. This exists alongside many hydrophobic interactions with various amino acid residues: Gly 116, Gly 117, Leu 22, Asp 21, Gly 17, Thr 146, Gly 20, Ser 59, Glu 30, Thr 56, Ala 9, Phe 31, Phe 34 and Tyr 121.

The interactions between almost all atoms in the compounds and amino acid residues of enzymes were recorded in (Table 6). Docking was performed for the Ligand and its complexes on the dihydrofolate reductase in a trial to predict their mode of action as anticancer drugs. The compounds show several interactions with dihydrofolate reductase enzyme. Particularly noteworthy are the Pd (II) Complex, which suggest that they might exert their action through inhibition of the DHFR enzyme.

Table 6: The interactions between almost all atoms in the compounds and amino acid residues of enzyme.

Compounds	S*	rmsd*	Ligand Interactions		
			Receptor	Interactions	Distance (Å)
Ligand	-6.1397	1.1419	ILE 7	H-donor	2.84
			ILE 16		2.88
Mn(II) Complex	-6.0592	3.0244		H-donor	
			VAL 115		2.95
Pd(II) Complex	-6.1085	0.8087	SER 59	H-donor	2.98

* rmsd: the root mean square deviation of the pose, in Å. S: the final energy score

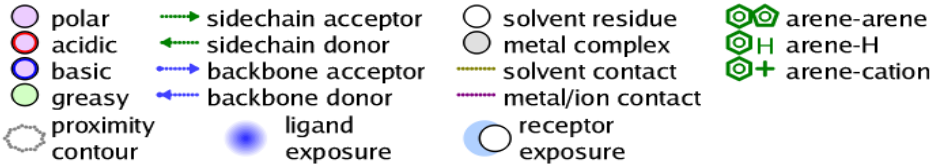

Figure 10: Scheme 2: The representative keys for the type of interaction between substrates and the enzyme

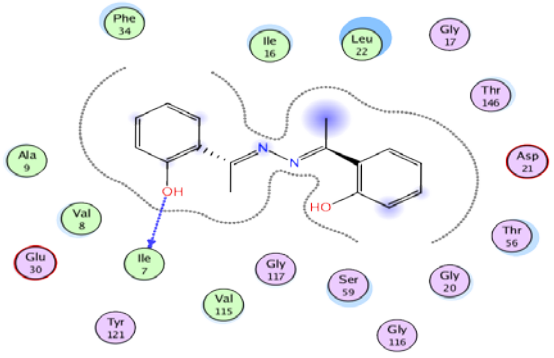

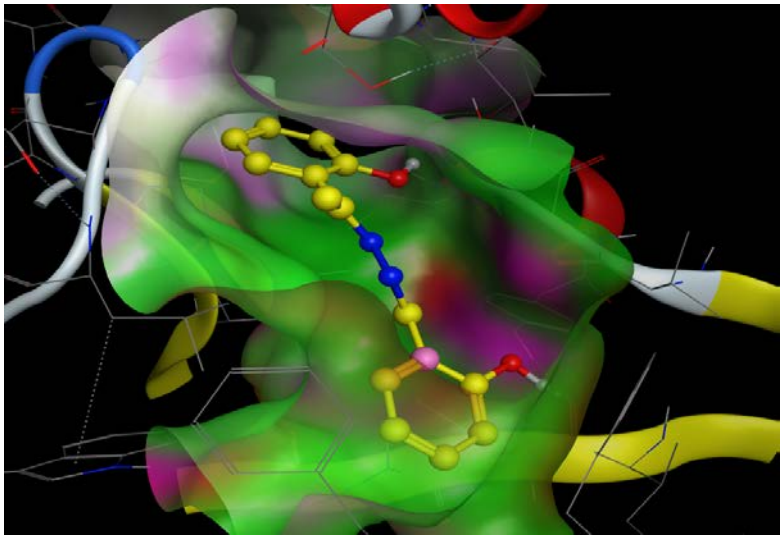

Figure 6: 2D Diagram and 3D Active site of docking of the Ligand into the dihydrofolate reductase (DHFR) enzyme

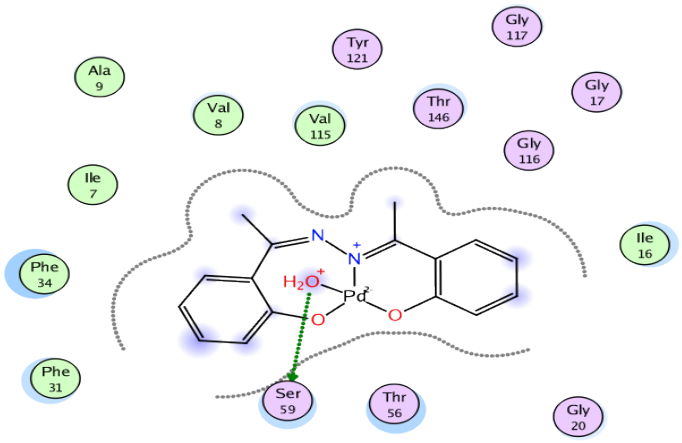

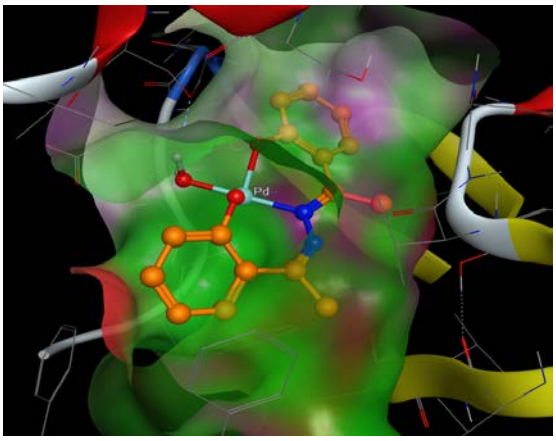

Figure 7: 2D Diagram and 3D Active site of docking of the Pd(II) complex into the dihydrofolate reductase (DHFR) enzyme

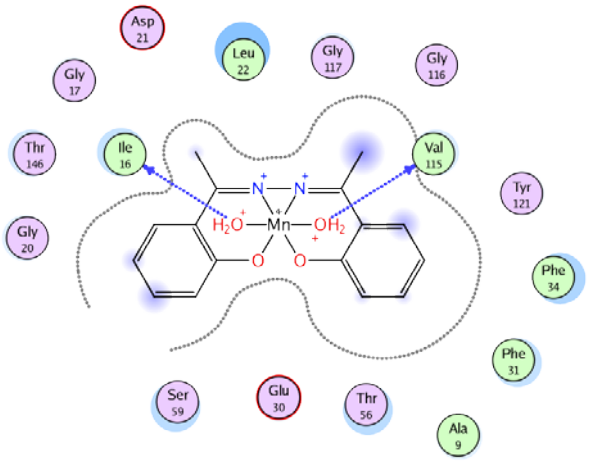

Figure 8: 2D Diagram and 3D Active site of docking of the Mn(II) complex into the dihydrofolate reductase (DHFR) enzyme

4. Conclusion

In the present work, we have studied the molecular structural of the synthesized orthohydroxyacetophenone azine ligand and its complexes with Pd(II) and Mn(II). Based on the results of spectroscopic data, the ligand reacts with metal ions as a 1:1 molar ratio. The coordination points are nitrogen of azomethine, phenolic oxygen and two of coordinated water. Octahedral geometry of Mn(II) complex it has been confirmed using UV-Vis, ESR spectra and magnetic moment. Thermal decomposition of the complexes shows the thermal stability of Mn metal up to 750°C compared with Pd metal which decomposed at the end of decomposition process. Active surface area(S) of the compounds by XRD data describe the highly surface activity of Pd(II) complexes compared with Mn(II) complex. Results of docking study for the samples with DHFR enzyme shows the highly effective of Pd(II) complex compared with other compounds in the inhibition of the enzyme

Acknowledgements

Our thanks go to Professor Dr. Badr Eldeen Awad El-Sayed Chemistry Department, Faculty of Science, Al Azhar University, Cairo, Egypt, for his effective contribution and Valuable help in the interpretation of some of the results.

References

[1]. J. Safari, S. Gandomi. "Structure, synthesis and application of azines: a historical perspective." Journal of Royal Society of Chemical, vol. 4, pp. 46224-46249, Sep. 2014.

[2]. A. H. Ammar, B. A. El-Said, E. A. El-Said. "Structural and optical studies on orthohydroxyacetophenone azine thin films." Journal of Materials Science, vol. 37, pp. 3255-3260, Aug. 2002.

[3]. D. Donnecke, G. Wunderia, W. Imhof. "Ligand properties of aromatic azines: C-Hactivation, metal induced disproportionation and catalytic C-C coupling reaction." Journal of Organometallic Chemistry, vol. 689, pp. 585-594, Feb. 2004.

[4]. S. Kulaksuzoglu, R. Gub. "A new bis (azine)tetradentate ligand and its transition metal complexes: synthesis, characterization and extraction properties." Journal of Chemical Papers, vol. 66, pp. 194-201, Mar. 2012.

[5]. C.-W. Sun, H.-F. Wang, J. Zhu, D.-R. Yang, J. Xing, J. Jin. "Novel symmetrical trans-bis-Schiff bases of N-substituted-4- piperidones: synthesis, characterization, and preliminary antileukemia activity mensurations." Journal of Heterocyclic Chemistry, vol. 50, pp. 1374–1380, Nov. 2013.

[6]. B. A. El- Sayed, M. M. Abo-Ali, M. S. Attia, S. Gamal. "Synthesis, spectroscopic characterization of palladium(II)-orthohydroxyacetophenone azine nano-optical sensor doped in sol–gel matrix and its use as probe for assessment of α-amylase activity in human saliva." Journal of Luminescence, vol. 169, pp. 99-105, Jan. 2016.

[7]. M. Shakir, S. Hanif, M. A. Sherwani, O. Mohammed, S. I. Al-Resayes. "Pharmacologically significant complexes of Mn(II), Co(II), Ni(II), Cu(II) and Zn(II) of novel Schiff base ligand, (E)-N-(furan-2-yl methylene) quinolin-8-amine: Synthesis, spectral, XRD, SEM, antimicrobial, antioxidant and in vitro cytotoxic studies". Journal of Molecular Structure, vol. 1092, pp. 143-159, Jul. 2015.

[8]. N. Kumar, G. Singh, A. K. Yadav. "Synthesis of some new pyrido [2, 3-d] pyrimidines and their ribofuranosides as possible antimicrobial agents." Heteroatom Chemistry, vol. 12, pp. 52-56, Jan. 2001.

[9]. G. Mangalagiu, M. Ungureanu, G. Grosu, I. Mangalagiu, M. Petrovanu. "New pyrrolo-py- rimidine derivatives with antifungal or antibacterial properties." Annales Pharmaceutiques Francaise, vol. 59, pp. 139-140, Apr. 2001.

[10]. J. W. De Boer, J. Brinkasma, W. R. Browne, A. Meetsma, P. L. Alsters, R. Hage, B. L. Feringa. "cis-Dihydroxylation and Epoxidation of Alkenes by $[Mn_2O(RCO_2)_2(tmtacn)_2]$: Tailoring the Selectivity of a Highly H_2O_2-Efficient Catalyst." Journal of American Chemical Society, vol. 127, pp. 7990-7991, May. 2005.

[11]. (a)Z. Guo, P. J. Sadler. "Metals in Medicine." Angewandte Chemie International Edition, vol. 38, pp. 1512-1531, May, 1999. (b)V. B. Arion, E. Reisner, M. Fremuth, M. A. Jakupec, B. K. Keppler, V. Y.

Kukushkin, A. J. L. Pombeiro. “Synthesis, X-ray diffraction structures, spectroscopic properties and in vitro antitumor activity of isomeric (1H-1, 2, 4-triazole) Ru(III) complexes.” Inorganic Chemistry, vol. 42, pp. 6024-6031, Aug. 2003.

[12]. L. V. Ababei, A. Kriza, C. Andronescu , A. M. Musuc. “Synthesis and characterization of new complexes of some divalent transition metals with 2-acetyl-pyridyl-isonicotinoylhydrazone.” Journal of Thermal Analysis and Calorimetry, vol. 107, pp. 107:573–584, Feb. 2012.

[13]. R. Kumar, M. Kaur, M. S. Bahia, O. Silakari. “Synthesis, cytotoxic study and docking based multidrug resistance modulator potential analysis of 2-(9-oxoacridin-10(9H)-yl)-N-phenyl acetamides.” European Journal of Medicinal Chemistry, vol. 80, pp. 83-91, Jun. 2014.

[14]. W. H. Xiao, G. J. Bennett. “Effects of mitochondrial poisons on the neuropathic pain produced by the chemotherapeutic agents, paclitaxel and oxaliplatin.” Pain, vol. 153, pp. 704-709, Jan. 2012.

[15]. E. S. E. El-Awady, Y. M. Moustafa, D. M. Abo-Elmatty, A. Radwan. “Cisplatin-induced cardiotoxicity: Mechanisms and cardioprotective strategies.” European Journal of Pharmacology, vol. 650, pp. 335-341, Jan. 2011.

[16]. K. A. Conklin. “Cancer chemotherapy and antioxidants.” Journal of Nutrition, vol. 134, pp. 3201S-3204S, Nov. 2004.

[17]. P. Arthi, S. Shobana, P. Srinivasan, L. Mitu, A. Kalilur Rahiman. “Synthesis, characterization, biological evaluation and docking studies of macrocyclic binuclear manganese (II) complexes containing 3,5-dinitrobenzoyl pendant arms.” Spectrochimica Acta Part A: Molecular and Biomolecular Spectroscopy, vol. 143, p. 49-58, May. 2015.

[18]. B. A. El-Sayed, M. M. Abo Aly, A. A. A. Emara, S. M. E. Khalil. “Synthesis and structural study of the ligand o-OH acetophenone azine and its Cu (II), Ni(II), Co(II) and Zn(II) complexes.” Journal of Vibrational Spectroscopy, vol. 30, pp. 93-100, Sep. 2002.

[19]. E. M. Nour, A. A. Taha, A. S. Al-Naimi. “Infrared and Raman studies of [UO_2 (salen)(L)](L= H_2O and CH_3OH).” Journal of Inorganica Chimica Acta, vol. 141, pp. 139-144, Jan. 1988.

[20]. B. A. El-Sayed, M. M. Abo Aly, G. M. Attia. “Vibrational and Electronic Studies on Salicylaldazine Transition Metal Complexes,” in Proc. of the Twelfth International Conference on FT Spectroscopy Tokyo, Japan, 1999, pp. 505-512.

[21]. M. M. Abo Aly, B. A. El-Sayed, A. M. Hassan. “Vibrational Spectra of Benzaldazine and Salicylaldazine Complexes with Zn (II) and Fe (II) Ions.” Journal of Spectroscopy Letters, vol. 35, pp. 337-348, Jul. 2002.

[22]. C. Anitha, C. D. Sheela, P. Tharmaraj, S. Johnson Raja. “Synthesis and characterization of VO(II), Co(II), Ni(II), Cu(II) and Zn(II) complexes of chromon based azo-linked Schiff base ligand.” Journal of Spectrochimica Acta Part A: Molecular and Biomolecular Spectroscopy, vol. 98, pp. 35-42, Dec. 2012.

[23]. F. A. Cotton, D. M. L. Goodgame, M. Goodgame. “Absorption spectra and electronic structure of some tetrahedral Manganese (II) complexes.” Journal of American Chemical Society, vol. 84, pp. 167-172, Jan. 1962.

[24]. F. A. Cotton, G. Wilkinson, C. A. Murillo, M. Bochmann. “Advanced Inorganic Chemistry”. John Wiley and Sons, New York, 1999, pp. 784-922.

[25]. A.W. Coats, J. P. Redfern. “Kinetic parameters from thermogravimetric data.” Nature. Vol. 201, pp. 68-69, Jan. 1964.

[26]. O. A. M. Ali. “Synthesis, spectroscopic, fluorescence properties and biological evaluation of novel Pd(II) and Cd(II) complexes of NOON tetradentate Schiff bases.” Spectrochimica Acta Molecular and Biomolecular Spectroscopy, vol. 121, pp. 188-195, May. 2014.

[27]. N. S. Abdel-Kader, R. M. Amin, A. L. El-Ansary. “Complexes of Schiff base of benzopyran-4-one derivative Synthesis, characterization, non-isothermal decomposition kinetics and cytotoxicity studies.” Journal of Thermal Analysis and Calorimetry, Vol. 123, pp. 1695–1706, Feb. 2016.

[28]. R. M. Issa, S. A. Amer, I. A. Mansour, A. I. Abdel-Monsef. **“**THERMAL STUDIES OF BIS SALICYLIDENE ADIPIC DIHYDRAZONE DERIVATIVES AND THEIR COMPLEXES WITH DIVALENT IONS OF Mn, Co, Ni, Cu AND Zn.” Journal of Thermal Analysis and Calorimetry, vol. 90, pp. 261-267, Oct. 2007.

[29]. S. P. Jiang, Z. Liu, H. L. Tang, M. Pan. “Synthesis and characterization of PDDA-stabilized Pt nanoparticles for direct methanol fuel cells.” Electrochimica Acta, vol.51, pp. 5721-5730, Aug. 2006.

[30]. E. F. Abo Zeid, D. S. Kim, H. S. Lee, Y. T. Kim. “Temperature dependence of morphology and oxygen reduction reaction activity for carbon-supported Pd–Co electrocatalysts.” Journal of Applied Electrochemistry, vol. 40, pp. 1917-1923, Jul. 2010.